

Headline Articles

Synthesis, Crystal Structures, and Electrical Properties of Anion Radical Salts of Novel Electron Acceptors, 2,6-Dicyanomethylene-4-oxo-2,6-dihydrocyclopentadithiophene (CPDT-TCNQ) and Its Diselenophene Analogue (CPDS-TCNQ), Having Three Electron-Withdrawing Groups

Shinji Tarutani[1,†] **and Kazuko Takahashi***[,1,2]

[1]Department of Chemistry, Graduate School of Science, Tohoku University, Sendai 980-8578

[2]Center for Interdisciplinary Research, Tohoku University, Sendai 980-8578

Received September 1, 2003; E-mail: tkazuko@cir.tohoku.ac.jp

Novel heterophene analogues of tetracyanodiphenoquinodimethane (TCNDQ) having three electron-withdrawing groups in one molecule, 2,6-dicyanomethylene-4-oxo-2,6-dihydrocyclopentadithiophene (CPDT-TCNQ: **1**) and 2,6-dicyanomethylene-4-oxo-2,6-dihydrocyclopentadiselenophene (CPDS-TCNQ: **2**), have been synthesized. CPDT-TCNQ and CPDS-TCNQ have a good coplanar conformation and have a fairly high electron-accepting ability due to the existence of the central carbonyl group in addition to the two terminal dicyanomethylene groups. The anion radical salts, $Me_4X(CPDT\text{-}TCNQ)_2$ (X = N, P, and As), $Et_4N(CPDT\text{-}TCNQ)_2$, and $Me_4X(CPDS\text{-}TCNQ)_2$ (X = P and As), showed a metallic conducting behavior ($\sigma_{rt} = 260$ to 42 $S\,cm^{-1}$) down to 130–255 K. In the crystal structures of $Me_4X(CPDT\text{-}TCNQ)_2$ (X = N, P, and As), which are isostructural with each other, the acceptor molecules form rigid and tight two-dimensional networks consisting of strong S···N and O···H inter-column contacts in the side-by-side direction. However, these salts have an extremely one-dimensional electronic structure along the stacking direction. This fact indicates that the chalcogen atoms in the acceptor molecules do not increase the dimensionality of the electronic structures of the anion radical salts; that property is significantly different from the role of chalcogen atoms of TTF or BEDT-TTF type donor molecules. The existence of the central carbonyl group in CPDT-TCNQ and in CPDS-TCNQ plays a very important role to give metallic anion radical salts due to the rigid conformation. The phase transition at 130 K on $Me_4N(CPDT\text{-}TCNQ)_2$ is regarded as $2k_F$ CDW instability. The origins of the phase transitions at 165 K for $Me_4P(CPDT\text{-}TCNQ)_2$ and 185 K for $Me_4As(CPDT\text{-}TCNQ)_2$ are regarded as $4k_F$ CDW. Thus the phase transition mechanisms of these salts are significantly different from each other, although the crystal structures are isostructural.

Since the discovery of metallic behavior of the charge-transfer (CT)-complex of tetrathiafulvalene (TTF) with tetracyanoquinodimethane (TCNQ),[1] active investigations have been continued toward the discovery of novel organic materials with unique electronic or magnetic properties. In these efforts, a large number of donor molecules have been synthesized and a number of molecular metals and superconductors have been developed so far.[2] However, acceptor-based molecular metals and superconductors are not so many[3] when compared with donor-based molecular metals and superconductors. This is mainly ascribed to the difficulty in the molecular design and synthesis of acceptor molecules giving single crystalline conducting salts. Incorporation of chalcogen atoms such as S or Se in donor molecules for organic conductors has already been proved to be very important for increasing the dimensionality of the electronic structures, since good intermolecular orbital overlaps induced by the diffused 3pπ or 4pπ orbitals of the heavy chalcogen atoms are possible not only in the stacking directions but also in the side-by-side directions. Stimulated by the many successful investigations of the donor-based organic conductors, challenging efforts have been performed to introduce hetero atoms or heavy chalcogen atoms in acceptor molecules. Yamashita and his co-workers clarified that TCNQ derivatives fused with 1,2,5-thiadiazole or selenadiazole rings form two-dimensional sheet-like networks by the S···NC contacts in the crystal structure of the neutral acceptor molecules.[4] Ogura, Otsubo, and their co-workers synthesized bithienoquinonoid isologues of TCNDQ as well as thieno[3,2-*b*]thienoquinonoid and dithieno[3,2-*b*:2′,3′-*d*]thienoquinonoid isologues of TCNQ.[5] These heterophene-TCNQ analogues showed small on-site Coulomb repulsion and afforded several highly conductive CT-complexes with electron donors such as hexamethyl-

† Present address: Research Department of Yoshida-Minami Factory of Fuji Photo Film Co. Ltd., Kawashiri Yoshida-cho, 4000, Haibara-gun, Shizuoka 421-0396

Published on the web March 12, 2004; DOI 10.1246/bcsj.77.463

enetetratellurafulvalene. However, it has not been clarified in these CT-complexes whether the conduction occurs on the acceptor column or not. We have synthesized heterophene-extended [3]radialene-type acceptors affording metallic CT-complexes with TTF and TTT.[6] A large negative thermoelectric power of $-55\ \mu V\ K^{-1}$ at room temperature and a constant thermoelectric power in the region of 300–200 K was obtained from the measurement of the temperature dependence of the thermoelectric power, indicating that the conduction carrier of the metallic complex with TTF is electrons.[7] More recently, Günther and Hünig's group synthesized thieno[3,2-*b*]thienoquinonoid isologues of *N*,*N*′-dicyanoquinone diimine (DCNQI). The dibromo derivative of the isologue gave a metallic CT-complex with TTF.[8]

In spite of these challenging investigations, the hetero-atom effect or chalcogen-atom effect on the dimensionality of the electrical structures of these acceptor-based organic conductors has not been well known so far, since the heteroquinonoid incorporated acceptor molecules so far synthesized seldom give good quality single crystalline anion radical salts, which are needed to investigate the crystal structures and electrical properties. To overcome this difficulty, we have designed and successfully synthesized new heterophene-type acceptor molecules, 2,6-dicyanomethylene-4-oxo-2,6-dihydrocyclopenta-[2,1-*b*;3,4-*b*′]dithiophene (CPDT-TCNQ) **1**[9] and 2,6-dicyanomethylene-4-oxo-2,6-dihydrocyclopenta[2,1-*b*;3,4-*b*′]diselenophene (CPDS-TCNQ) **2**, as shown in Chart 1. These new acceptors **1** and **2** with three electron-withdrawing groups showed fairly high electron-accepting abilities and have highly rigid and coplanar conformations. These new acceptors gave one-dimensional metallic anion radical salts; we have thus clarified the hetero-atom effect of the acceptor molecules on conducting properties and crystal structures of the metallic salts. These are the first examples of metallic anion radical salts of the heterophene-TCNQ and heterophene-DCNQI families.

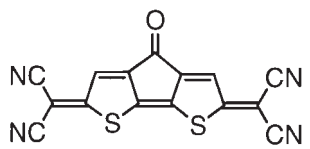

CPDT-TCNQ: **1**

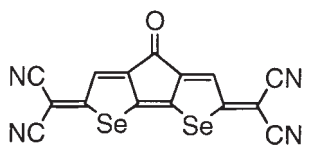

CPDS-TCNQ: **2**

Chart 1. Chemical structural formulas of CPDT-TCNQ and CPDS-TCNQ.

Results and Discussion

Synthesis. CPDT-TCNQ was synthesized according to the routes outlined in Scheme 1. The ketal **3**[10] was first lithiated with butyllithium and then allowed to react with 2 equiv of iodine to give the diiodo derivative **4** in 56% yield. Reaction of **4** with sodium dicyanomethanide in the presence of a catalytic amount of $[Pd(PPh_3)_4]$ in THF and subsequent oxidation with bromine afforded **5** in 74% yield. Deketalation of **5** with 70% perchloric acid in dichloromethane gave CPDT-TCNQ (**1**) as a stable violet powder in 96% yield. CPDS-TCNQ (**2**) was synthesized according to the routes shown in Scheme 2. 3-Bromoselenophene[11] was first lithiated with butyllithium and then allowed to react with the 3-formylselenophene to give the carbinol **6** in 80% yield. Oxidation of **6** with chromium trioxide in pyridine afforded the ketone **7** in 99% yield. Reaction of **7** with ethylene glycol in the presence of a catalytic amount of *p*-toluenesulfonic acid in benzene gave the ketal **8** in 98% yield. The ketal **8** was lithiated with 2 equiv of *t*-butyllithium to give 2,2′-dilithio derivative, which was allowed to react with iodine to give **9** in 79% yield. Intramolecular Ullmann coupling of the diiodo derivative **9** with copper powder in DMF gave **10** in 85% yield. The diiodo derivative **11** was obtained in 97% yield by the direct iodination of **10** with NIS in acetonitrile, since 2,5-dilithiation of **10** with *n*- or *t*-butyllithium was unsuccessful. The compound **11** was allowed to react with sodium dicyanomethanide in the presence of a catalytic amount of $[Pd(PPh_3)_4]$ in THF at 50 °C for 2 h and then at 60 °C for 2 h to give the dicyanomethylene derivative **12** in 63% yield. All reagents used for this dicyanomethylation must be fresh and completely dried. It is important to fulfill the reaction temperature and the reaction time exactly, since when the reaction was performed at 60 °C for 4 h, the yield of **12** decreases to 41%. Deketalation of **12** with 70% perchloric acid in dichloromethane gave CPDS-TCNQ (**2**) as a stable violet powder in 99% yield. CPDT-TCNQ and CPDS-TCNQ exhibited strong absorption maxima at 520 and 524 nm with absorption coefficients of $\log \varepsilon = 4.93$ and 4.86, respectively, as shown in Fig. 1.

Redox Properties. CPDT-TCNQ is reduced reversibly in three successive one-electron transfer processes to give the stable anion radical, dianion, and trianion radical species, this was demonstrated by the cyclic voltammograms showing three pairs of single-electron redox waves with a good reversibility, as shown in Fig. 2(a). The cyclic voltammogram of CPDS-TCNQ showed irreversible waves when measured in a usual scan speed of $50\ mV\ s^{-1}$ because of the low solubility of its

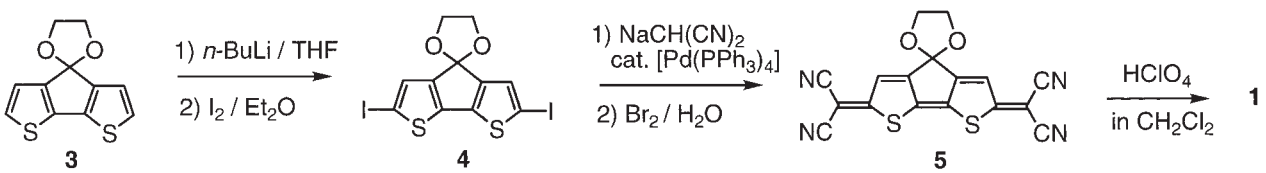

Scheme 1. Synthetic route of CPDT-TCNQ.

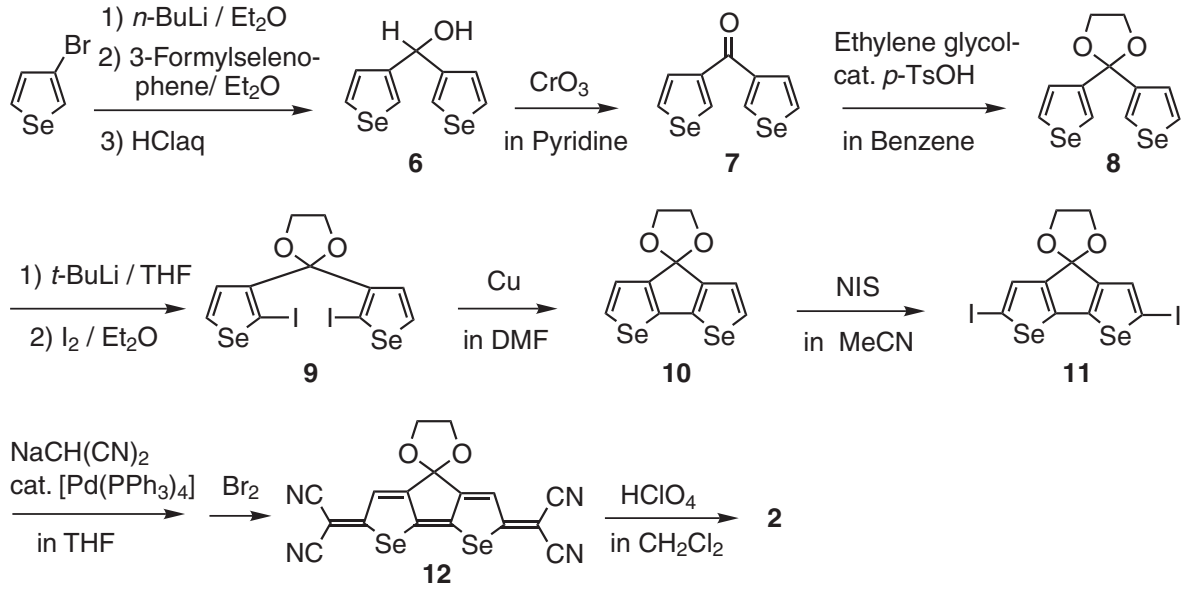

Scheme 2. Synthetic route of CPDS-TCNQ.

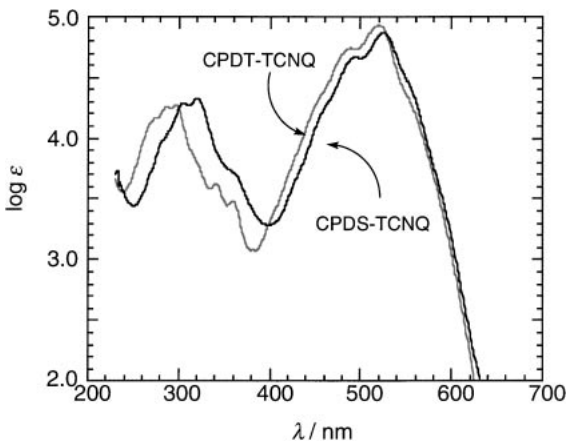

Fig. 1. UV–vis spectra of CPDT and CPDS in dichloromethane.

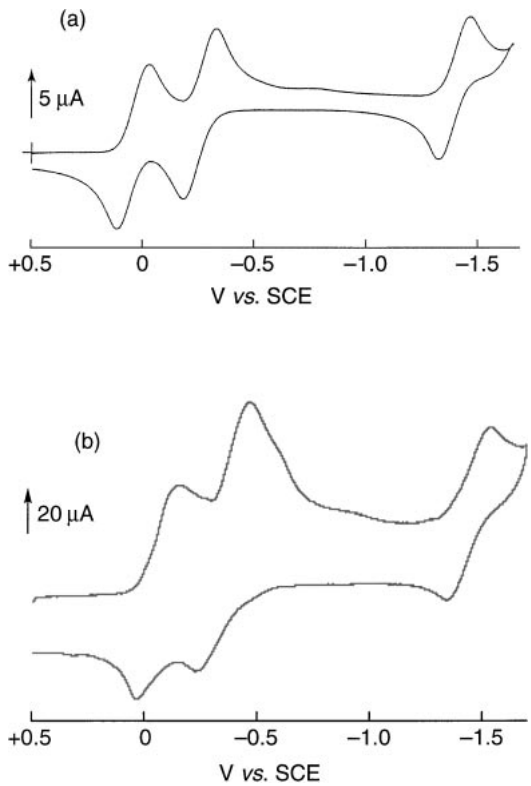

Fig. 2. Cyclic voltammograms of (a) CPDT-TCNQ (scan rate: 50 mV s^{-1}) and (b) CPDS-TCNQ (scan rate: 1.0 V s^{-1}) in dichloromethane under argon at room temperature (1.0 mM solution with 0.1 M TBAP).

anion radical species in dichloromethane. However, the reversible waves were observed at a rapid scan speed of 1.0 V s^{-1} as shown in Fig. 2(b). The half wave reduction potentials of CPDT-TCNQ, CPDS-TCNQ, and the ketal **5** as a reference compound are summarized in Table 1. The first reduction potential of CPDT-TCNQ is more positive by 0.18 V than that of the ketal **5** (−0.14 V), although it is more negative by 0.18 V than that of TCNQ (+0.22 V). The $\log K_{sem}$ value[12] of CPDT-TCNQ is larger by 1.36 than that of **5**, indicating that the anion radical of CPDT-TCNQ is thermodynamically stabilized by the delocalization of the unpaired electron over the three electron-accepting groups. The first reduction potential of CPDS-TCNQ is more negative by 0.10 V than that of CPDT-TCNQ. This can be ascribed to the larger energetic benefit in affording the anion radical of CPDT-TCNQ rather than in affording the anion radical of CPDS-TCNQ, since the central five-membered heterocyclic rings are aromatized in the anion radical state and the aromaticity of the thiophene ring is larger than that of the selenophene ring.

Electrical Properties of the Anion Radical Salts. The anion radical salts of CPDT-TCNQ and CPDS-TCNQ were prepared by electrochemical reduction in an H-type cell under the conditions listed in Table 2. Stoichiometries (C:A) and conducting properties of the anion radical salts are also listed in Table 2. From the 1:2 stoichiometry of these salts, the formal charge on CPDT-TCNQ and CPDS-TCNQ is determined to

Table 1. Reduction Potentials[a] of CPDT-TCNQ, CPDS-TCNQ, and **5**

Compound	E_1^{red}	E_2^{red}	E_3^{red}	ΔE ($E_1^{red} - E_2^{red}$)	log K_{sem}
CPDT-TCNQ	+0.04	−0.27	−1.43	0.31	5.26
CPDS-TCNQ	−0.06[b]	−0.35[b]	−1.45[b]	0.29	4.92
5	−0.14	−0.37	—	0.23	3.90

a) V vs SCE, 50 mV s^{-1}, 1.0 mM in CH_2Cl_2. b) V vs SCE, 1.0 V s^{-1}, 1.0 mM in CH_2Cl_2.

Table 2. Electrochemical Reduction and Conducting Properties of Anion Radical Salts of CPDT-TCNQ and CPDS-TCNQ

Acceptor	Electrolyte	Solvent	Current /μA	Period /day	Cation	C:A	$\sigma_{r.t.}$[a] /S cm^{-1}	σ_{max}[a] /S cm^{-1}	Enhancement[b]	$T_{\sigma max}$[c] /K	T_{MI}[d] /K
CPDT-TCNQ	Me_4NBF_4	Acetone	0.3	7	Me_4N	1:2[e]	160	170	1.06	250	130
	Me_4PClO_4	Acetone	0.3	7	Me_4P	1:2[e]	47	55	1.17	220	165
	Me_4AsClO_4	Acetone	0.3	7	Me_4As	1:2[e]	42	55	1.31	175	185
	Me_4SbClO_4	Acetone	0.3	7	Me_4Sb	1:2[e,f]	33	—	—	—	—
	Et_4NClO_4	Acetone	0.3	7	Et_4N	1:2[g]	260	310	1.19	210	212
CPDS-TCNQ	Me_4NBF_4	MeCN	0.3	6	Me_4N	1:2[g]	0.85[h]	—	—	—	—
	Me_4PClO_4	MeCN	0.3	6	Me_4P	1:2[g]	110	118	1.07	260	145
	Me_4AsClO_4	MeCN	0.3	6	Me_4As	1:2[g]	140	150	1.07	260	160
	Et_4NClO_4	MeCN	0.3	6	Et_4N	1:2[g]	2.4[h]	—	—	—	—

a) Measured by the four probe method on a single crystal. b) The ratio of σ_{max} to $\sigma_{r.t.}$. c) The temperature showing the maximum conductivity. d) The metal–insulator transition temperature. e) Determined by X-ray crystal structure analysis. f) This salt contains an acetone molecule. g) Determined by the elemental analysis. h) Measured by the four probe method on a compressed pellet.

be −0.5. These salts exhibited fairly high conductivities of 0.85–260 S cm^{-1} at room temperature. $Me_4X(CPDT\text{-}TCNQ)_2$ (X = P and As), $Et_4N(CPDT\text{-}TCNQ)_2$, and $Me_4X(CPDS\text{-}TCNQ)_2$ (X = P and As) showed the metallic temperature dependence of the resistivity. $Me_4Sb(CPDT\text{-}TCNQ)_2$(Acetone) and $R_4N(CPDS\text{-}TCNQ)_2$ (R = Me and Et) showed semiconducting temperature dependence of the resistivity. As shown in Fig. 3(a), the resistivity of a single crystal of $Me_4N\text{-}(CPDT\text{-}TCNQ)_2$ is almost steady from room temperature down to 130 K. Fairly small activation energies of $E_{a_1} = 100$ meV and $E_{a_2} = 83$ meV for the Me_4N salt at the temperature below 130 K were obtained from the Arrhenius plots of the temperature dependence of the resistivity as shown in Fig. 3(b). The metallic property of the Me_4N salt from room temperature down to 130 K was confirmed by the temperature dependence of the magnetic susceptibility measurement using a SQUID susceptometer, as shown in Fig. 4. The magnetic susceptibilities are invariable from room temperature down to the diamagnetic transition temperature ($T_{DIA} = 130$ K), which are regarded as Pauli-like, and decrease drastically at this temperature with the transition to the diamagnetic phases. The Peierls type transition is suggested for the Me_4N salt since the metal–insulator transition temperature ($T_{MI} = 130$ K)[13] is almost identical with the T_{DIA}. Indeed, as has been reported in the preceding paper, we observed superlattice formation of 0,2*b*,0 below 130 K in the X-ray oscillation photograph of the Me_4N salt, indicating that the M–I transition at 130 K is caused by a $2k_F$ CDW instability.[14] $Et_4N(CPDT\text{-}TCNQ)_2$ is also metallic down to 212 K, as shown in Fig. 5. The T_{MI} of the Et_4N salt is higher by 82 K than that of the Me_4N salt.

The temperature dependence of the resistivity and the $d(R_T/R_{300\,K})/dT$ vs T plot of $Me_4P(CPDT\text{-}TCNQ)_2$ are shown in Figs. 6(a) and (b), respectively, indicating that the M–I transition occurred at 165 K. The conducting property of

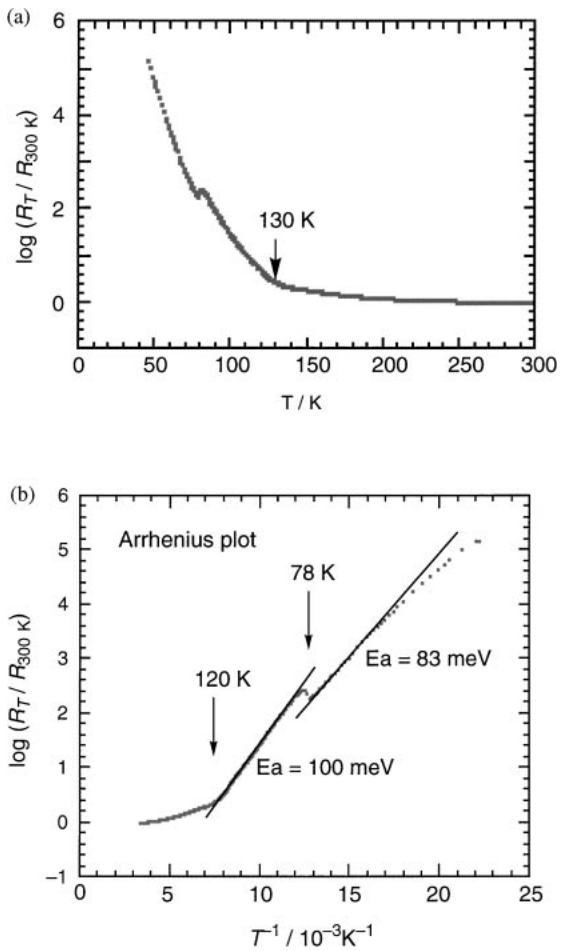

Fig. 3. Temperature dependence of the resistivity (a) and Arrhenius plot (b) for $Me_4N(CPDT\text{-}TCNQ)_2$.

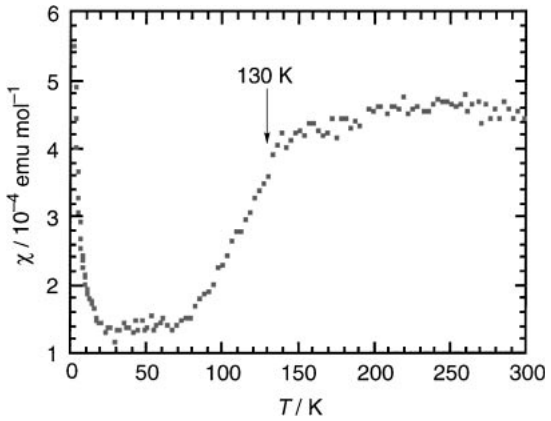

Fig. 4. Temperature dependence of the magnetic susceptibility of $Me_4N(CPDT\text{-}TCNQ)_2$.

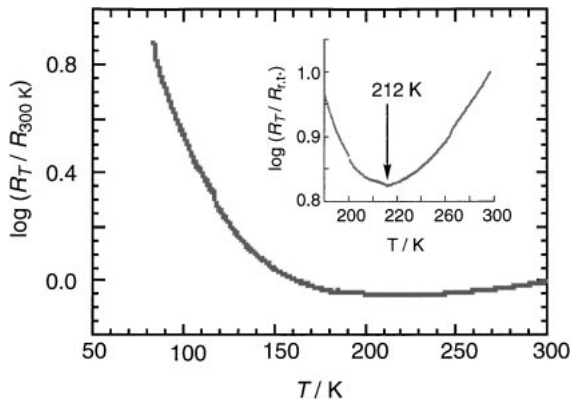

Fig. 5. Temperature dependence of the resistivity for $Et_4N(CPDT\text{-}TCNQ)_2$.

$Me_4As(CPDT\text{-}TCNQ)_2$ at low temperature closely resembles that of the Me_4P salt, demonstrating that the MI transition occurred at 185 K, as shown in Figs. 7(a) and (b). Interestingly, the magnetic susceptibility of the Me_4As salt does not decrease at the M–I transition temperature and a drastic decrease in the magnetic susceptibility occurred below 50 K as shown in Fig. 8. Moreover, the magnitude of the magnetic susceptibility (8×10^{-4} emu mol^{-1}) (Fig. 8) is relatively large when compared with those of ordinary molecular metals.[2a,b] This phenomenon suggests the existence of a $4k_F$ CDW growing phase at the temperature region between 185 K (T_{MI}) and 50 K (T_{DIA}) in the Me_4As salt. We observed superlattice formations of $2a$,0,0 below 165 K for the Me_4P salt and of $2a$,0,0 below 185 K for the Me_4As salt in the X-ray oscillation photographs, indicating that the origins of the M–I transitions at 165 K and at 185 K are $4k_F$ CDW instabilities.[14] The $4k_F$ CDW instabilities are probably coupled with the cation ordering at the transition temperature, since the Me site of the cation radical is ordered below the transition temperature, while the Me site is statically disordered above the transition temperature; this was revealed by the low temperature crystal structure analysis that included the superspot for the Me_4As salt.[14]

The temperature dependences of the resistivity for $Me_4N(CPDS\text{-}TCNQ)_2$ and $Et_4N(CPDS\text{-}TCNQ)_2$ were measured on a compressed pellet because their crystals are too thin to connect the gold wires. Both salts showed the semiconducting temperature dependences of the resistivity with small activation energies of $E_a = 37$ meV for the Me_4N salt and $E_a = 34$ meV for the Et_4N salt at around room temperature. Taking into consideration their small E_a values on the compressed pellets measurements, one may conclude that their single crystals may show a metallic behavior.

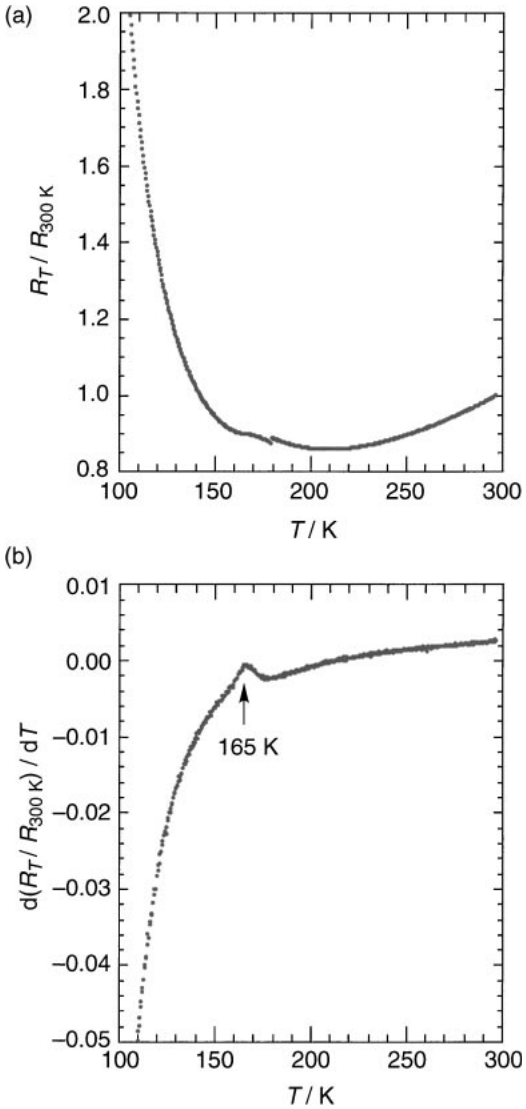

Fig. 6. Temperature dependence of the resistivity (a) and $d(R_T/R_{300\,K})/dT$ vs T plot (b) for $Me_4P(CPDT\text{-}TCNQ)_2$.

The temperature dependence of the resistivity and the $d(R_T/R_{300\,K})/dT$ vs T plot of $Me_4P(CPDS\text{-}TCNQ)_2$ are shown in Figs. 9(a) and (b), respectively, indicating that the M–I transition occurred at 145 K. The temperature dependence of the resistivity and the $d(R_T/R_{300\,K})/dT$ vs T plot of $Me_4As(CPDS\text{-}TCNQ)_2$ are shown in Figs. 10(a) and (b), respectively, indicating that the M–I transition occurred at 160 K. The origins of the M–I transitions of $Me_4P(CPDS\text{-}TCNQ)_2$ and $Me_4As(CPDS\text{-}TCNQ)_2$ are not clarified yet, since the single crystals are not suitable for submitting to X-ray photography.

Crystal Structures of the Anion Radical Salts. Molecular and crystal structures of $Me_4X(CPDT\text{-}TCNQ)_2$ (X = N, P, and

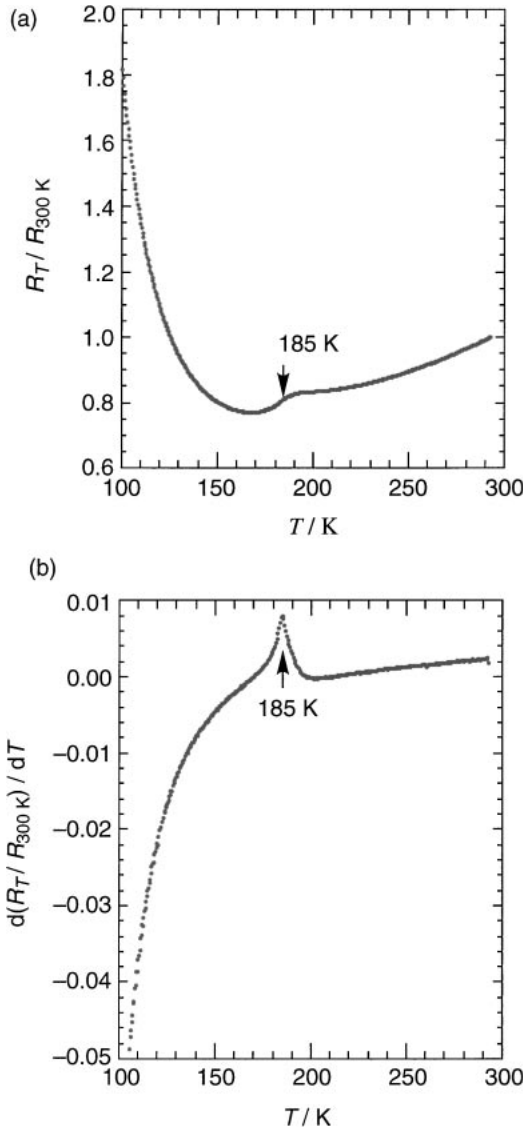

Fig. 7. Temperature dependence of the resistivity (a) and $d(R_T/R_{300\,K})/dT$ vs T plot (b) for $Me_4As(CPDT\text{-}TCNQ)_2$.

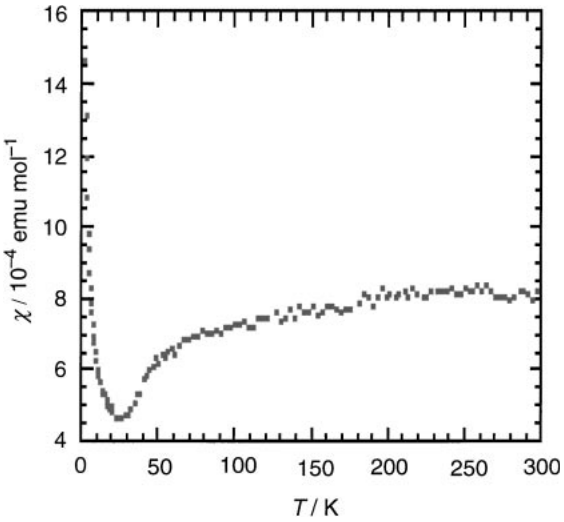

Fig. 8. Temperature dependence of the magnetic susceptibility of $Me_4As(CPDT\text{-}TCNQ)_2$.

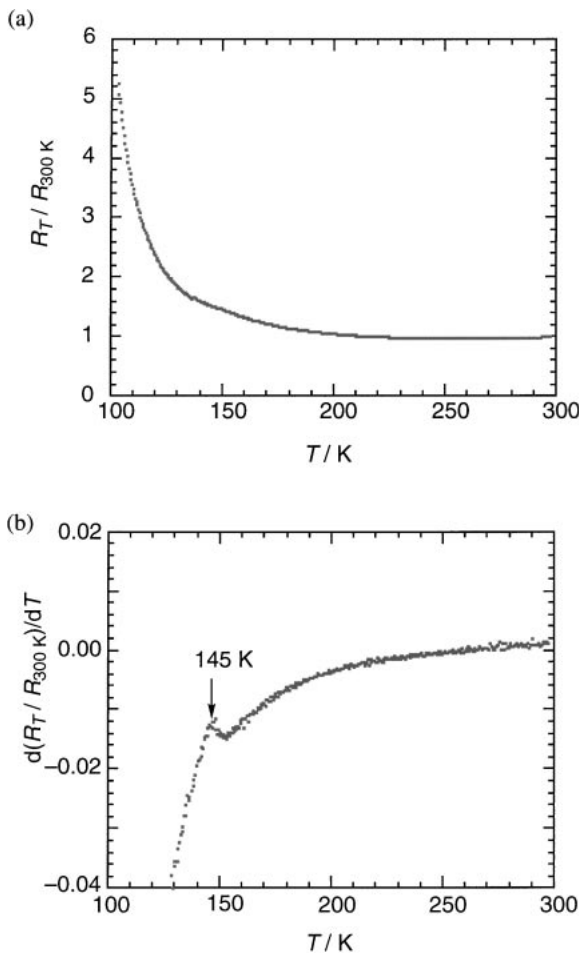

Fig. 9. Temperature dependence of the resistivity (a) and $d(R_T/R_{300\,K})/dT$ vs T plot (b) for $Me_4P(CPDS\text{-}TCNQ)_2$.

As) and $Me_4Sb(CPDT\text{-}TCNQ)_2$(Acetone) were elucidated by X-ray crystallographic analyses. The crystal structures of the metallic salts $Me_4X(CPDT\text{-}TCNQ)_2$ (X = N, P, and As) are isostructural with each other, as shown in Table 3. The single crystals of these three salts belong to the monoclinic system and to the space group of $P2/n$. The unit cell contains four crystallographically equivalent acceptor molecules and two cations, giving a cation to acceptor ratio of 1:2. The acceptor molecule retains a good coplanar conformation. The unit cell contains two acceptor columns stacking along the *b*-axis; each column is separated by a cation layer, as shown in Fig. 11(a). The acceptor columns in these three salts are constituted by the weakly dimerized CPDT-TCNQ molecules (Table 4) with intra-dimer interplanar distances of 3.20–3.21 Å (c1 in Fig. 12) and inter-dimer interplanar distances of 3.32–3.33 Å (c2 in Fig. 12). The overlapping mode of the acceptor molecules is the so-called ring-over-ring type in the intra-dimer overlap (Fig. 13(a)) and is the so-called ring-over-bond type in the inter-dimer overlap (Fig. 13(b)). Interestingly, there are two S1···N2 (3.01–2.99 Å) and two S2···N2 (3.04–2.99 Å) contacts which are shorter than the sum of van der Waals radii of sulfur and nitrogen atoms (3.40 Å), and there are two short intermolecular hydrogen bonds between O1···H11 (2.26–2.32 Å) which is

Table 3. Crystal Data of Anion Radical Salts of CPDT-TCNQ

Cation	Me_4N	Me_4P	Me_4As	Me_4Sb[a)]
C:A	1:2	1:2	1:2	1:2
Crystal system	monoclinic	monoclinic	monoclinic	triclinic
Space group	$P2/n$	$P2/n$	$P2/n$	$P1$
Z	4	4	4	1
a/Å	7.4763(7)	7.446(2)	7.430(2)	7.4898(5)
b/Å	6.9411(7)	6.984(2)	6.994(2)	18.013(2)
c/Å	30.428(4)	31.596(2)	31.922(2)	6.9745(6)
α/deg	—	—	—	96.013(8)
β/deg	91.523(10)	92.33(2)	92.50(2)	90.979(6)
γ/deg	—	—	—	86.795(7)
R	0.062	0.035	0.034	0.059
R_w	0.067	0.038	0.036	0.064

a) This salt contains one acetone molecule per unit.

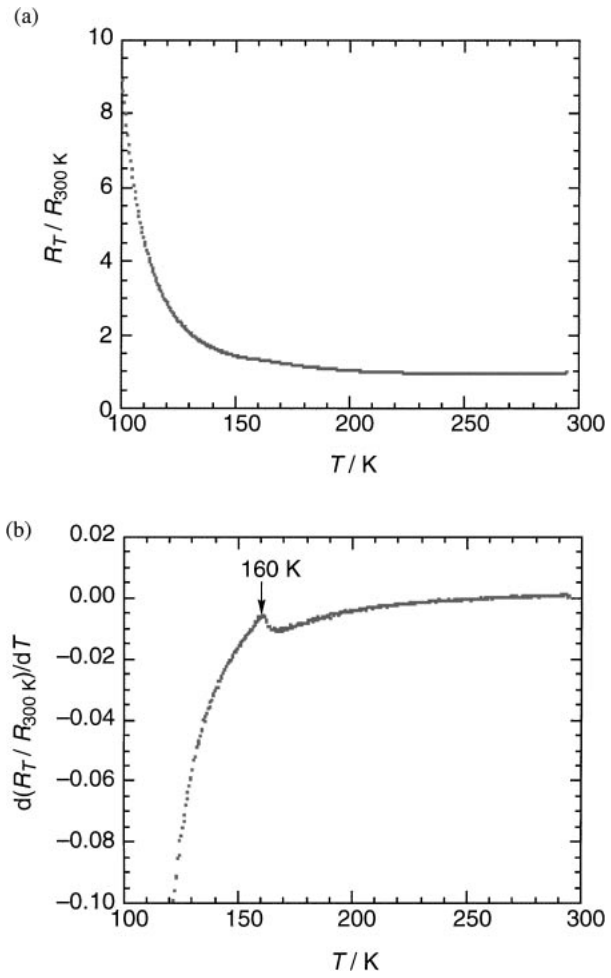

Fig. 10. Temperature dependence of the resistivity (a) and $d(R_T/R_{300\,K})/dT$ vs T plot (b) for $Me_4As(CPDS\text{-}TCNQ)_2$.

shorter than the sum of van der Waals radii of oxygen and hydrogen atoms (2.70 Å), along the acceptor short axis in the crystal structures of these salts, as shown in Fig. 14 and Table 5. Thus rigid and tight two-dimensional layered intermolecular networks are constructed along the *ab*-plane for Me_4X-$(CPDT\text{-}TCNQ)_2$ (X = N, P, and As).

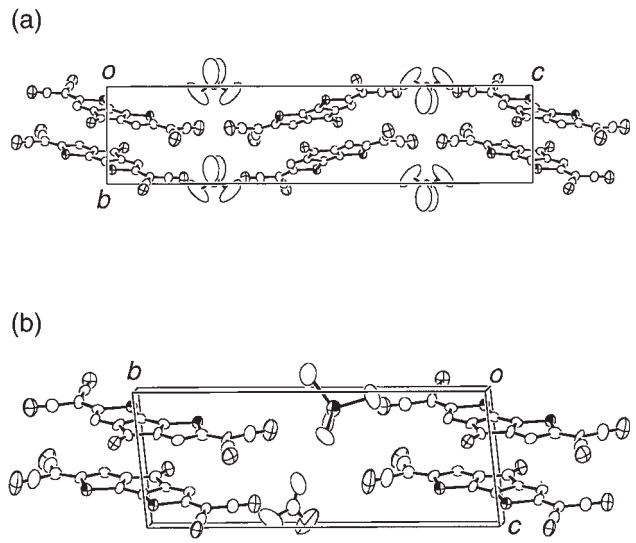

Fig. 11. Crystal structures of (a) $Me_4N(CPDT\text{-}TCNQ)_2$ and (b) $Me_4Sb(CPDT\text{-}TCNQ)_2$ projection onto the *bc*-plane.

Table 4. Interplanar Distances (Å) of CPDT-TCNQ Salts

Cation	Me_4N	Me_4P	Me_4As	Me_4Sb
Intra-dimer (c1)	3.20	3.21	3.21	3.23
Inter-dimer (c2)	3.32	3.33	3.33	3.34

The single crystal of $Me_4Sb(CPDT\text{-}TCNQ)_2$(Acetone) belongs to the triclinic system and to the space group of $P1$ (Table 3). There are two crystallographically independent acceptor molecules (A and B) which stack along the *c*-axis in an A–B–A–B manner and in a face-to-face manner, directing alternately the central carbonyl group to the opposite side. The unit cell of the Me_4Sb salt (Fig. 11(b)) contains two acceptor molecules (A and B), one cation, and one acetone molecule (solvent), giving a cation to acceptor ratio of 1:2. The unit cell contains one acceptor column stacking along the *c*-axis and each column is separated by a cation layer. Since there are no great differences in bond lengths and bond angles between

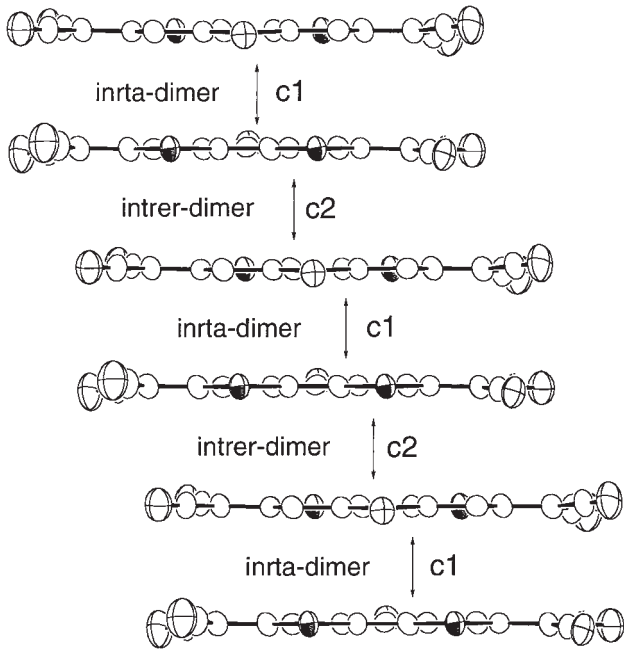

Fig. 12. Stacking mode of the acceptor molecules of $Me_4N(CPDT\text{-}TCNQ)_2$.

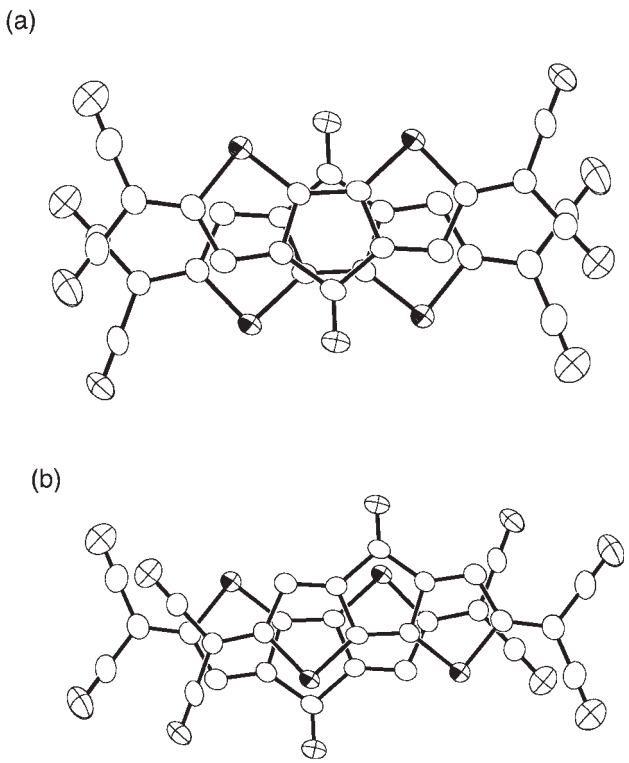

Fig. 13. Overlapping modes of acceptor molecules in $Me_4N(CPDT\text{-}TCNQ)_2$: (a) intra-dimer overlap, (b) inter-dimer overlap.

the two molecules A and B in the Me_4Sb salt, as shown in Fig. 15, the overlapping modes of the acceptor molecules in the stacking column and the mode of the hetero-atom contacts in the side-by-side direction in the Me_4Sb salt are essentially conformable with those of the Me_4N, Me_4P, and Me_4As salts.

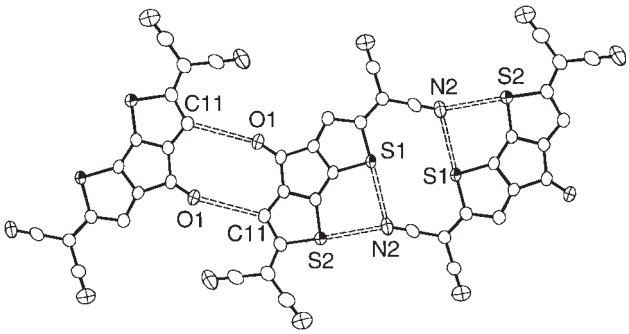

Fig. 14. Side-by-side interactions of the acceptor molecules in $Me_4N(CPDT\text{-}TCNQ)_2$.

Table 5. Hetero-Atom Contacts (Å) in Side-by-Side Direction in Anion Radical Salts of CPDT-TCNQ

Cation	Me_4N	Me_4P	Me_4As	Me_4Sb
S1···N2	3.01	3.03	2.99	2.97
S2···N2	3.04	2.99	3.03	3.03
O1···C11	3.28	3.25	3.24	3.28
O1···H11	2.26	2.32	2.26	2.39

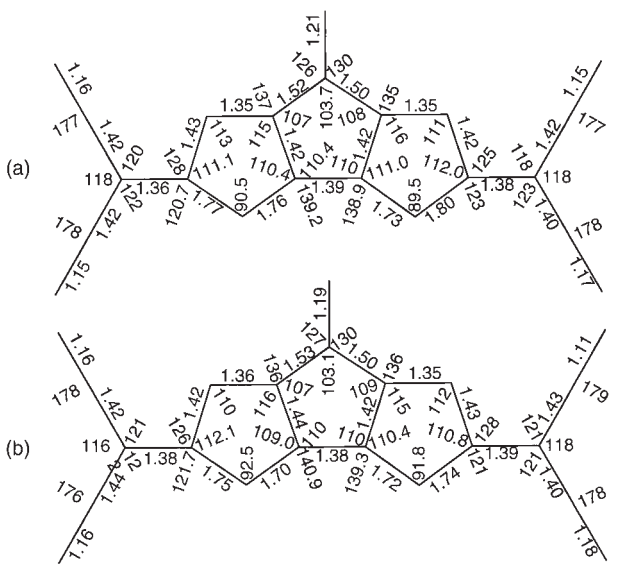

Fig. 15. Bond lengths and bond angles of the acceptor molecules of $Me_4Sb(CPDT\text{-}TCNQ)_2$: (a) molecule A, (b) molecule B.

Thus the rigid and tight two-dimensional layered intermolecular networks are constructed along the *ac*-plane for $Me_4Sb(CPDT\text{-}TCNQ)_2$(Acetone). The interplanar distances, c1 and c2, and intermolecular hetero-atom contacts of the Me_4Sb salt are almost identical with those of the other monoclinic salts, as shown in Tables 4 and 5.

Band Structures. The intermolecular overlap integrals of $Me_4X(CPDT\text{-}TCNQ)_2$ (X = N, P, and As) and Me_4Sb-$(CPDT\text{-}TCNQ)_2$(Acetone) calculated by the extended Hückel method on the basis of the molecular and the crystal structures obtained by X-ray crystal analysis are summarized in Table 6. There is no significant difference between c1 and c2, indicating

Table 6. Calculated Intermolucular Overlap Integrals[a] ($S \times 10^3$) of Anion Radical Salts of CPDT-TCNQ

Cation	Me_4N	Me_4P	Me_4As	Me_4Sb
c1 (intra-dimer)	−19.65	−18.83	−18.83	−18.66
c2 (inter-dimer)	16.53	14.37	15.14	15.65
a	0.0744	0.0559	0.0713	−0.0137
p (S···N contact)	0.00429	0.0913	0.00393	−0.0627
q (hydrogen bond)	0.00672	0.0104	0.026	0.00693

a) The overlap modes, c1, c2, a, p, and q, are indicated in Fig. 16.

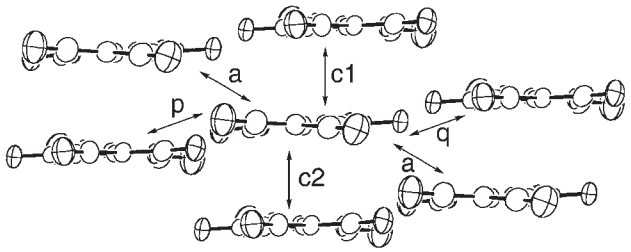

Fig. 16. Molecular arrangement of the acceptor molecules of $Me_4N(CPDT\text{-}TCNQ)_2$ viewed along the acceptor short axis.

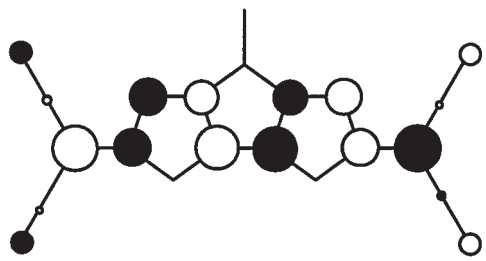

Fig. 17. The π-AO coefficients in the LUMO of CPDT-TCNQ obtained from MINDO, PM-3 calculation.

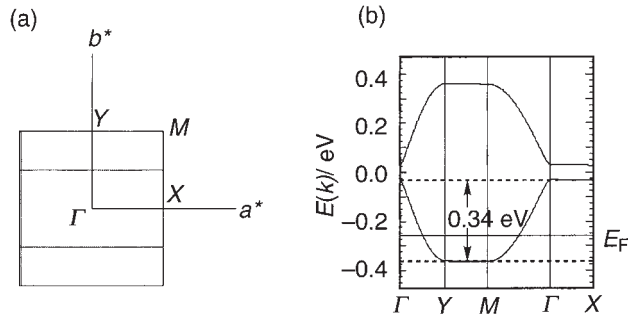

Fig. 18. Fermi surface (a) and band structure (b) of $Me_4N(CPDT\text{-}TCNQ)_2$ calculated by the tight binding approximation method.

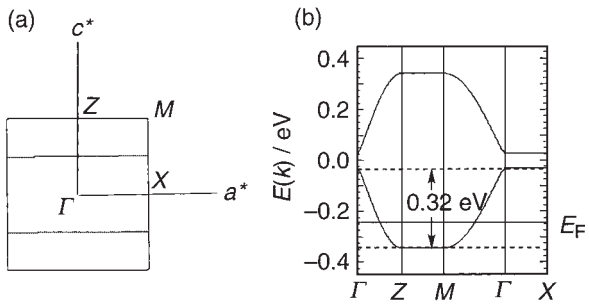

Fig. 19. Fermi surface (a) and band structure (b) of $Me_4Sb(CPDT\text{-}TCNQ)_2$(Acetone) calculated by the tight binding approximation method.

that the degree of the dimerization is very weak in these salts. On the other hand, the overlap integrals along the side-by-side direction are less than 1/300 of the values of c1 or c2, in spite of the existence of the inter-column S···N and O···H contacts in the side-by-side direction. The extremely small overlap integrals along the side-by-side direction are ascribed to the extremely small π-atomic orbital coefficients of the O and the S atoms in the LUMO of CPDT-TCNQ molecules shown in Fig. 17. The tight-binding band calculations[15] using the overlap integrals shown in Table 6 demonstrate that these salts have highly one-dimensional Fermi surfaces opened along the a^*-axis, as shown in Fig. 18(a). The solvent-free Me_4Sb salt, if it is accessible, may show a metallic behavior, since the Fermi surface of the Me_4Sb salt does not significantly differ from those of the Me_4N, Me_4P, and Me_4As salts, as shown in Fig. 19(a). The main reason for the non-metallic behavior of the Me_4Sb salt may be the crystal defects due to the loss of acetone molecules during the resistivity measurement. These four salts have a split band structure due to their dimerized crystal structures; the lower energy band is half filled, as shown in Fig. 18(b) and Fig. 19(b). The calculated band widths are 0.73, 0.67, 0.68, and 0.69 eV in the Me_4N, Me_4P, Me_4As, and Me_4Sb salts, respectively. As described previously, the origin of the phase transition of the Me_4N salt at 130 K is $2k_F$ CDW, whereas the origins of the phase transitions of the Me_4P and Me_4As salts are $4k_F$ CDW. The occurrence of the $2k_F$ CDW instability in the Me_4N salt can be explained by the relatively large band width of 0.73 eV for the Me_4N salt, since metals with a large band width can obtain a large energy benefit by forming the Peierls-type band gap.

Conclusion

Novel heterophene-TCNQ type acceptors with three electron-withdrawing groups in one molecule, CPDT-TCNQ and CPDS-TCNQ, were synthesized. Anion radical salts of CPDT-TCNQ and CPDS-TCNQ showed metallic behavior. These are the first examples of molecular metals of the heterophene-TCNQ family. The crystal structures of the metallic salts, $Me_4X(CPDT\text{-}TCNQ)_2$ (X = N, P, and As), are isostructural with each other. The acceptor columns are connected by the side-by-side S···N and O···H contacts constructing a rigid

and tight two-dimensional molecular network. In spite of the two-dimensional molecular network, Fermi surfaces of these metallic salts are extremely one-dimensional. This is ascribed to the extremely small π-atomic orbital coefficients of the O and the S atoms in the LUMO of CPDT-TCNQ. Thus, one of the next targets to obtain acceptor-based two-dimensional metallic conductors would be the synthesis of new acceptor molecules carrying large π-atomic coefficients on the skeletal hetero-atoms in the LUMO of the acceptors. From the experimental results of this study and from the result of the preceding study,[14] the phase transition mechanisms of the present extremely one-dimensional molecular metals were clarified. The origin of the phase transition in $Me_4N(CPDT\text{-}TCNQ)_2$ is $2k_F$ CDW. On the other hand, the origins of the phase transitions in $Me_4X(CPDT\text{-}TCNQ)_2$ (X = P and As) are $4k_F$ CDW. The occurrence of the $2k_F$ CDW in the Me_4N salt can be ascribed to the relatively large band width of this salt, since metals with a large band width can obtain a large energy benefit by forming the Peierls-type band gap.

Experimental

General. All melting points were determined by a Yanagimoto micro melting point apparatus and are not corrected. All of the chemicals and solvents were purified and completely dried before use. NMR spectra were recorded on a Bruker AC-200P spectrometer. ^{1}H NMR and ^{13}C NMR chemical shifts were recorded relative to TMS as internal standard. Chemical shift assignments were confirmed through spin decoupling and two-dimensional carbon–proton chemical shift correlation experiments. IR spectra were recorded on a HORIBA FT-300 spectrometer. MS spectra were recorded on either a JEOL-JMS-HX-110 or a HITACHI-M-2500S spectrometer. Elemental analyses were performed at the Instrumental Analysis Center for Chemistry, Tohoku University. The cyclic voltammograms were taken on a BAS CV-50W under argon atmosphere at room temperature. The conductivities of the anion radical salts were measured by the four probe method on using a YOKOGAWA 7651 programmable direct current source and a KEITHLEY 2001 digital multimeter unit on a single crystal except for the Me_4N and Et_4N salts of CPDS-TCNQ which were measured on a compressed pellet. Gold wires (10 or 15 μm diameter) were attached to the single crystal or to the pellet with carbon paste. The magnetic property measurements were carried out with a commercial superconducting quantum interference (SQUID) magnetrometer manufactured by Quantum Design Co. Ltd. (MPMS2 and MPMS-XL). The X-ray diffraction data were collected by using a Rigaku AFC5R four-circle diffractometer with Cu Kα radiation monochromatized by graphite (λ(Cu Kα) = 1.54178 Å, ω–2θ scans) at a temperature of 13 ± 1 °C. The structures were solved by the direct method (SIR 92) and refined by the full-matrix least-squares method. The non-hydrogen atoms were refined anisotropically. Some hydrogen atoms were refined isotropically. The rest were included in fixed positions. All calculations were performed using the teXsan crystallographic software package of Molecular Strucuture Corporation. Crystallographic data have been deposited at the CCDC, 12 Union Road, Cambridge CB2 1EZ, UK and copies can be obtained on request, free of charge, by quoting the publication citation and the deposition numbers CCDC 224213–224216.

4-Ethylenedioxy-2,6-diiodocyclopenta[2,1-*b*;3,4-*b*′]dithiophene (4). To a solution of 4-ethylenedioxycyclopenta[2,1-*b*;3,4-*b*′]dithiophene **3**[10] (2.80 g, 11.8 mmol) in anhydrous THF (130 mL) was added dropwise a hexane solution of butyllithium (1.64 M solution, 21.7 mL, 35.5 mmol) with stirring at −40 °C under argon atmosphere; then the reaction mixture was warmed to 0 °C and stirred for 30 min. To this was added dropwise a solution of iodine (9.02 g, 35.5 mmol) in anhydrous ether (70 mL) at −78 °C, and the reaction mixture was allowed to warm to room temperature and was then stirred for 30 min. The reaction mixture was poured into aqueous Na_2SO_3, and extracted with dichloromethane. The dichloromethane extract was washed successively with water and then brine, and then was dried over Na_2SO_4. Solvent evaporation from the extract gave a residue, which was washed with dichloromethane (25 mL) to remove easily soluble impurities to give **4** as a crude product (4.00 g). To the dichloromethane washings was added hexane (25 mL), and the resulting solution was chromatographed on silica gel by eluting with dichloromethane–hexane (1:1) to give a further amount of the crude product **4** (589 mg). Recrystllization of the combined crude product from benzene–ethanol (2:3) gave pure 4-ethylenedioxy-2,6-diiodocyclopenta[2,1-*b*;3,4-*b*′]dithiophene (**4**) as yellow needles (3.23 g, 6.61 mmol, 56%): mp 256–258 °C; ^{1}H NMR ($CDCl_3$, 200 MHz) δ 7.11 (2H, s, H-4), 4.26 (4H, s, OCH_2CH_2O); IR (KBr) 3087, 2991, 2972, 2897, 1485, 1427, 1406, 1346, 1302, 1203, 1188, 1153, 1018, 982, 947, 845, 820 cm^{-1}; UV (MeCN) λ/nm (log ε) 396 (sh, 3.84), 368 (4.20), 256 (sh, 4.00), 244 (4.24); MS (DEI, 70 eV) *m*/*z* (rel intensity) 491 ($M^+ + 3$, 1.55), 490 ($M^+ + 2$, 11.47), 489 ($M^+ + 1$, 15.57), 488 (M^+, 100), 444 ($M^+ - C_2H_4O$, 2.69), 361 ($M^+ - I$, 56.39), 317 ($M^+ - C_2H_4O - I$, 17.11). Found: C, 26.81; H, 1.29; I, 52.12%. Calcd for $C_{11}H_6I_2O_2S_2$: C, 27.07; H, 1.24; I, 52.00%.

2,6-Dicyanomethylene-4-ethylenedioxy-2,6-dihydrocyclopenta[2,1-*b*;3,4-*b*′]dithiophene (5). To a suspension of sodium hydride (55–65 wt %, 492 mg, about 12 mmol) in anhydrous THF (25 mL) was added dropwise a solution of malononitrile (541 mg, 8.19 mmol) in anhydrous THF (25 mL) with stirring at room temperature under argon atmosphere; then the reaction mixture was stirred for 10 min at room temperature. To this were added successively a solution of **4** (1.00 g, 2.05 mmol) in anhydrous THF (25 mL) and [Pd(PPh_3)$_4$] (474 mg, 0.410 mmol). The mixture was refluxed for 4 h, cooled to room temperature, and then poured into a solution of bromine (15 mL) in water (150 mL). The resulting precipitate was collected by filtration, washed with water and then with acetone, to give almost pure 2,6-dicyanomethylene-4-ethylenedioxy-2,6-dihydrocyclopenta[2,1-*b*;3,4-*b*′]dithiophene **5** (546 mg, 1.51 mmol, 74%), which was purified by sublimation in vacuo (10^{-3} mmHg, 300 °C) giving pure **5** as a violet powder: mp > 300 °C; IR (KBr) 3059, 2897, 2218, 1508, 1352, 1325, 1217, 1126, 1032, 1005, 949, 870, 768 cm^{-1}; UV–vis (CH_2Cl_2) λ/nm (log ε) 525 (4.92), 495 (4.87), 463 (4.59), 362 (3.04), 345 (3.27), 330 (3.21), 276 (3.67), 262 (3.83); MS (DEI, 70 eV) *m*/*z* (rel intensity) 365 ($M^+ + 3$, 2.74), 364 ($M^+ + 2$, 11.29), 363 ($M^+ + 1$, 23.08), 362 (M^+, 100), 318 ($M^+ - C_2H_4O$, 16.70). Found: C, 55.97; H, 1.90; N, 15.52%. Calcd for $C_{17}H_6N_4O_2S_2$: C, 56.34; H, 1.67; N, 15.46%.

2,6-Dicyanomethylene-4-oxo-2,6-dihydrocyclopenta[2,1-*b*;3,4-*b*′]dithiophene (CPDT-TCNQ). To a suspension of finely powdered **5** (100 mg, 0.276 mmol) in dichloromethane (100 mL) was added 70% perchloric acid (15 mL) at 0 °C. The reaction mixture was stirred vigorously for 3 h at 0 °C, and then poured into ice-water. The resulting mixture was extracted with dichloromethane. The dichloromethane extract was washed in sequence with saturated aqueous $NaHCO_3$, water, and then brine, and was then dried over Na_2SO_4. Solvent evaporation gave a crude product (107

mg). This was chromatographed on silica gel by eluting with dichloromethane to give 2,6-dicyanomethylene-4-oxo-2,6-dihydrocyclopenta[2,1-*b*;3,4-*b*′]dithiophene (CPDT-TCNQ) (84.2 mg, 0.624 mmol, 96%), which was purified by sublimation in vacuo (10^{-3} mmHg, 300 °C) giving pure CPDT-TCNQ as a violet powder: mp > 300 °C; IR (KBr) 3047, 2218, 1732, 1504, 1460, 1325, 1252, 1225, 957, 897, 760 cm^{-1}; UV–vis (CH_2Cl_2) λ/nm (log ε) 553 (sh, 4.32), 520 (4.93), 489 (4.74), 458 (sh, 4.37), 360 (3.48), 341 (3.62), 323 (sh, 3.75), 314 (sh, 3.89), 297 (4.27), 286 (4.26), 274 (4.16); MS (DEI, 70 eV) *m*/*z* (rel intensity) 321 ($M^+ + 3$, 2.23), 320 ($M^+ + 2$, 11.47), 319 ($M^+ + 1$, 19.38), 318 (M^+, 100); HRMS *m*/*z* 317.9673 (M^+) (Calcd for $C_{15}H_2N_4OS_2$: 317.9670). Found: C, 56.22; H, 1.01; N, 17.39%. Calcd for $C_{15}H_2N_4OS_2$: C, 56.60; H, 0.63; N, 17.60%.

Bis(3-selenienyl)methanol (6). To a solution of 3-bromoselenophene[11] (3.98 g, 18.7 mmol) in anhydrous ether (40 mL) was added dropwise a hexane solution of butyllithium (1.68 M solution, 11.2 mL, 18.7 mmol) with stirring at −78 °C over a period of 20 min; then the reaction mixture was stirred for 1 h at −78 °C under argon atmosphere. To this was added dropwise a solution of 3-selenophenecarbaldehyde[16] (2.98 g, 18.7 mmol) in anhydrous ether (40 mL) with stirring at −78 °C over a period of 30 min, and the reaction mixture was stirred for 1 h at −78 °C. After being warmed to room temperature, the reaction mixture was poured into 1 M hydrochloric acid and extracted with ether. The ether extract was washed with water and then with brine, and dried over Na_2SO_4. Solvent evaporation from the extract gave a residue which was chromatographed on basic alumina by eluting with chloroform to give a crude product (5.23 g). Further recrystallization from hexane gave pure bis(3-selenienyl)methanol **6** as colorless fine needles (4.35 g, 15.0 mmol, 80%): mp 77–79 °C; ^{1}H NMR ($CDCl_3$, 200 MHz) δ 7.97 (2H, dd, $J_{5,4} = 5.44$ Hz, $J_{5,2} = 2.52$ Hz, H-5), 7.88 (2H, ddd, $J_{2,5} = 2.52$ Hz, $J_{2,4} = 1.31$ Hz, $J_{2,\underline{C}H\underline{O}H} = \sim 1.0$ Hz, H-2), 7.30 (2H, dd, $J_{4,5} = 5.44$ Hz, $J_{4,2} = 1.31$ Hz, H-4), 5.88 (1H, br.s, C<u>H</u>OH), 2.22 (1H, br.s, CHO<u>H</u>); ^{13}C NMR ($CDCl_3$, 50 MHz) δ 146.7 (C-3), 131.0 (C-5), 129.2 (C-4), 126.3 (C-2), 71.4 (CHOH); IR (KBr) 3219, 3105, 3080, 2895, 1431, 1292, 1269, 1203, 1115, 1078, 1030, 945, 899, 822, 779, 758, 700, 681, 654 cm^{-1}; UV–vis (MeCN) λ/nm (log ε) 256 (4.18), 231 (sh, 3.89); MS (DEI, 70 eV) *m*/*z* (rel intensity) 294 ($M^+ + 2$, 8.26), 292 (M^+, 28.83), 291 ($M^+ - 1$, 5.95), 290 ($M^+ - 2$, 26.62), 289 ($M^+ - 3$, 11.80), 288 ($M^+ - 4$, 16.29), 287 ($M^+ - 5$, 16.29), 286 ($M^+ - 6$, 6.75), 273 ($M^+ - H_2O - 1$, 6.35), 211 ($M^+ - Se - 1$, 19.89), 195 ($M^+ - OH - Se$, 9.67), 183 ($M^+ - COH$, 10.22), 159 (C_4H_3SeCO, 100), 133 ($C_4H_4Se + 1$, 60.33); HRMS *m*/*z* 291.8903 (M^+) (Calcd for $C_9H_8OSe_2$: 291.8956). Found: C, 37.27; H, 2.89%. Calcd for $C_9H_8OSe_2$: C, 37.27; H, 2.78%.

Bis(3-selenienyl) Ketone (7). To a suspension of chromium trioxide (4.34 g, 43.4 mmol) in anhydrous pyridine (42 mL) was added dropwise a solution of **6** (4.20 g, 14.5 mmol) in anhydrous pyridine (42 mL) with stirring at 0 °C over a period of 30 min; then the reaction mixture was stirred for 36 h at room temperature under argon atmosphere. The inorganic precipitate was removed by filtration and the filtrate was poured into 6 M hydrochloric acid and extracted with chloroform. The chloroform extract was washed successively with aqueous $NaHCO_3$ solution, water, and then brine, and dried over Na_2SO_4. Solvent evaporation gave a crude product (4.15 g) which was chromatographed on silica gel by eluting with chloroform to give bis(3-selenienyl) ketone **7** (4.11 g, 14.3 mmol, 99%). Further recrystallization from ethanol gave pure **7** as colorless needles. When aqueous acetic acid was used instead of pyridine as the solvent, the yield of **7** dropped significantly. Compound **7**: mp 101–102 °C; ^{1}H NMR ($CDCl_3$, 200 MHz) δ 8.75 (2H, dd, $J_{2,5} = 2.42$ Hz, $J_{2,4} = 1.24$ Hz, H-2), 8.06 (2H, dd, $J_{5,4} = 5.51$ Hz, $J_{5,2} = 2.42$ Hz, H-5), 7.87 (2H, dd, $J_{4,5} = 5.51$ Hz, $J_{4,2} = 1.24$ Hz, H-4); ^{13}C NMR ($CDCl_3$, 50 MHz) δ 184.5 (CO), 144.7 (C-3), 139.7 (C-2), 131.2 (C-5), 130.5 (C-4); IR (KBr) 3107, 3087, 3064, 1624, 1537, 1512, 1475, 1427, 1383, 1346, 1255, 1151, 1099, 996, 899, 825, 798, 731, 708, 679 cm^{-1}; UV–vis (MeCN) λ/nm (log ε) 289 (4.27), 260 (sh, 4.11), 230 (sh, 4.16), 226 (4.17), 203 (4.31); MS (DEI, 70 eV) *m*/*z* (rel intensity) 292 ($M^+ + 2$, 8.61), 291 ($M^+ + 1$, 3.91), 290 (M^+, 33.41), 289 ($M^+ - 1$, 4.78), 288 ($M^+ - 2$, 28.03), 287 ($M^+ - 3$, 11.37), 286 ($M^+ - 4$, 15.65), 285 ($M^+ - 5$, 4.61), 284 ($M^+ - 6$, 7.53), 262 ($M^+ - CO$, 4.03), 209 ($M^+ - Se - 1$, 3.76), 182 ($M^+ - Se - CO$, 4.48), 159 ($M^+ - C_4H_3Se$, 100), 131 (C_4H_3Se, 47.67); HRMS *m*/*z* 289.8757 (M^+) (Calcd for $C_9H_6OSe_2$: 289.8749). Found: C, 37.53; H, 2.31%. Calcd for $C_9H_6OSe_2$: C, 37.53; H, 2.10%.

2,2-Bis(3-selenienyl)-1,3-dioxolane (8). A solution of **7** (4.10 g, 14.2 mmol), *p*-toluenesulfonic acid monohydrate (271 mg, 1.43 mmol), and ethylene glycol (7.94 mL, 142 mmol) in benzene (200 mL) was heated to reflux under a Dean-Stark head for 24 h under argon atmosphere. After being cooled to room temperature, the reaction mixture was poured into aqueous $NaHCO_3$ and extracted with toluene. The toluene extract was washed with water and with brine, and then dried over Na_2SO_4. Solvent evaporation gave a crude product, which was chromatographed on basic alumina by eluting with toluene to give 2,2-bis(3-selenienyl)-1,3-dioxolane **8** (4.65 g, 14.0 mmol, 98%). Further recrystallization from ethanol gave pure **8** as colorless prisms: mp 133–134 °C; ^{1}H NMR ($CDCl_3$, 200 MHz) δ 7.98 (2H, dd, $J_{2,5} = 2.50$ Hz, $J_{2,4} = 1.29$ Hz, H-2), 7.94 (2H, dd, $J_{5,4} = 5.41$ Hz, $J_{5,2} = 2.50$ Hz, H-5), 7.37 (2H, dd, $J_{4,5} = 5.41$ Hz, $J_{4,2} = 1.29$ Hz, H-4), 4.08 (4H, s, OCH_2CH_2O); ^{13}C NMR ($CDCl_3$, 50 MHz) δ 145.5 (C-3), 130.7 (C-2), 129.1 (C-4), 128.0 (C-5), 101.6 (OCO), 65.0 (OCH_2CH_2O); IR (KBr) 3097, 3074, 2974, 2945, 2881, 1537, 1433, 1223, 1163, 1066, 1024, 1007, 982, 947, 901, 872, 804, 766, 702, 671 cm^{-1}; UV–vis (MeCN) λ/nm (log ε) 254 (4.21) 228 (sh, 3.87); MS (DEI, 70 eV) *m*/*z* (rel intensity) 336 ($M^+ + 2$, 5.24), 334 (M^+, 16.36), 332 ($M^+ - 2$, 13.19), 331 ($M^+ - 3$, 5.98), 330 ($M^+ - 4$, 8.43), 328 ($M^+ - 6$, 3.17), 262 ($M^+ - C_3H_4O_2$, 6.21), 203 ($M^+ - C_4H_3Se$, 100), 159 (C_4H_3SeCO, 46.01); HRMS *m*/*z* 333.9020 (M^+) (Calcd for $C_{11}H_{10}O_2Se_2$: 333.9011). Found: C, 39.76; H, 3.33%. Calcd for $C_{11}H_{10}O_2Se_2$: C, 39.78; H, 3.03%.

2,2-Bis(2-iodo-3-selenienyl)-1,3-dioxolane (9). To a solution of **8** (4.60 g, 13.9 mmol) in anhydrous THF (120 mL) was added dropwise a pentane solution of *t*-butyllithium (1.64 M solution, 20.3 mL, 33.2 mmol) with stirring at −78 °C over a period of 20 min under argon atmosphere; then the reaction mixture was stirred for 1 h at −78 °C. To this was added dropwise a solution of iodine (9.84 g, 38.8 mmol) in anhydrous ether (60 mL) at −78 °C over a period of 30 min, and the reaction mixture was stirred for 30 min at −78 °C. After being warmed to room temperature, the reaction mixture was poured into aqueous Na_2SO_3, and extracted with chloroform. The chloroform extract was washed with water and with brine, and then dried over Na_2SO_4. Solvent evaporation gave a crude product (8.03 g) which was recrystallized from benzene to give 2,2-bis(2-iodo-3-selenienyl)-1,3-dioxolane **9** as colorless plates (6.38 g, 10.0 mmol, 79%): mp 181–183 °C; ^{1}H NMR ($CDCl_3$, 200 MHz) δ 8.05 (2H, d, $J_{5,4} = 6.09$ Hz, H-5), 7.21 (2H, d, $J_{4,5} = 6.09$ Hz, H-4), 4.12 (4H, s, OCH_2CH_2O); ^{13}C NMR ($CDCl_3$, 50 MHz) δ 146.3 (C-3), 135.5 (C-5), 132.1 (C-4), 108.0 (OCO), 75.5 (C-2), 65.1 (OCH_2CH_2O); IR (KBr) 3095, 3068, 2991, 2937, 2887, 1464, 1410, 1234, 1215, 1190, 1132, 1113,

1074, 1011, 955, 916, 891, 810, 785, 715, 681 cm^{-1}; UV–vis (MeCN) λ/nm (log ε) 259 (4.31); MS (DEI, 70 eV) m/z (rel intensity) 589 ($M^+ + 3$, 1.76), 588 ($M^+ + 2$, 12.22), 587 ($M^+ + 1$, 5.48), 586 (M^+, 41.21), 585 ($M^+ - 1$, 6.62), 584 ($M^+ - 2$, 35.43), 583 ($M^+ - 3$, 14.01), 582 ($M^+ - 4$, 22.28), 581 ($M^+ - 5$, 6.01), 580 ($M^+ - 6$, 7.79), 579 ($M^+ - 7$, 2.02), 578 ($M^+ - 8$, 1.85), 459 ($M^+ - I$, 10.54), 329 ($M^+ - C_4H_2SeI + 1$, 100), 285 ($M^+ - C_4H_2SeI - C_2H_4O_2 + 1$, 29.90); HRMS m/z 585.6944 (M^+) (Calcd for $C_{11}H_8I_2O_2Se_2$: 585.6952). Found: C, 22.92; H, 1.45%. Calcd for $C_{11}H_8I_2O_2Se_2$: C, 22.62; H, 1.38%.

4-Ethylenedioxycyclopenta[2,1-*b*;3,4-*b*′]diselenophene (10). A suspension of **9** (6.00 g, 10.3 mmol) and copper powder (2.09 g, 32.9 mmol) in anhydrous DMF (60 mL) was heated to reflux for 3 h under argon atmosphere. After being cooled to room temperature, the inorganic precipitate was filtered and washed with chloroform. The filtrate and the chloroform washings were poured into aqueous $NaHCO_3$, and extracted with chloroform. The chloroform extract was washed with water and with brine, and then dried over Na_2SO_4. Solvent evaporation gave a residue which was chromatographed on silica gel by eluting with toluene to give a crude product (3.09 g). Further recrystallization from ethanol–benzene (1:1) gave 4-ethylenedioxycyclopenta[2,1-*b*;3,4-*b*′]diselenophene (**10**) as colorless plates (2.88 g, 8.72 mmol, 85%): mp 159–160 °C; ^{1}H NMR ($CDCl_3$, 200 MHz) δ 7.81 (2H, d, $J_{5,4} = 5.37$ Hz, H-5), 7.18 (2H, d, $J_{4,5} = 5.37$ Hz, H-4), 4.30 (4H, s, OCH_2CH_2O); ^{13}C NMR ($CDCl_3$, 50 MHz) δ 151.2 (C-2), 144.7 (C-3), 131.8 (C-5), 123.4 (C-4), 108.8 (OCO), 65.2 (OCH_2CH_2O); IR (KBr) 3093, 2964, 2897, 1728, 1496, 1481, 1423, 1377, 1353, 1296, 1246, 1221, 1152, 1078, 1012, 982, 943, 895, 856, 822, 762, 712, 675 cm^{-1}; UV–vis (MeCN) λ/nm (log ε) 356 (3.93), 278 (sh, 3.84), 269 (3.89), 243 (3.96), 234 (sh, 3.88); MS (DEI, 70 eV) m/z (rel intensity) 334 ($M^+ + 2$, 32.19), 333 ($M^+ + 1$, 12.44), 332 (M^+, 100), 331 ($M^+ - 1$, 14.84), 330 ($M^+ - 2$, 82.76), 329 ($M^+ - 3$, 34.98), 328 ($M^+ - 4$, 51.30), 327 ($M^+ - 5$, 14.45), 326 ($M^+ - 6$, 19.63), 302 ($M^+ - CH_2O$, 20.55), 288 ($M^+ - C_2H_4O$, 16.83), 272 ($M^+ - C_2H_4O_2$, 46.69); HRMS m/z 331.8859 (M^+) (Calcd for $C_{11}H_8O_2Se_2$: 331.8855). Found: C, 40.03; H, 2.32%. Calcd for $C_{11}H_8O_2Se_2$: C, 40.02; H, 2.44%.

4-Ethylenedioxy-2,6-diiodocyclopenta[2,1-*b*;3,4-*b*′]diselenophene (11). To a solution of **10** (600 mg, 1.82 mmol) in anhydrous acetonitrile (30 mL) was added a solution of NIS (1.02 g, 4.54 mmol) in anhydrous acetonitrile (15 mL) with stirring at room temperature under argon atmosphere. Then, the reaction mixture was stirred for 5 min at room temperature, poured into aqueous $NaHCO_3$, and the resulting solution was extracted with chloroform. The chloroform extract was washed successively with aqueous Na_2SO_3, water, and brine, and was dried over Na_2SO_4. Solvent evaporation gave a crude product which was chromatographed on silica gel by eluting with toluene to give 4-ethylenedioxy-2,6-diiodocyclopenta[2,1-*b*;3,4-*b*′]diselenophene **11** (1.02 g, 1.76 mmol, 97%). Further recrystallization from ethanol gave pure **11** as yellow needles: mp > 300 °C (decomp at 165 °C); ^{1}H NMR ($CDCl_3$, 200 MHz) δ 7.38 (2H, s, H-4), 4.26 (4H, s, OCH_2CH_2O); ^{13}C NMR ($CDCl_3$, 50 MHz) δ 151.1 (C-2), 149.6 (C-3), 133.2 (C-4), 107.9 (OCO), 76.0 (C-5), 65.4 (OCH_2CH_2O); IR (KBr) 2956, 2877, 1726, 1475, 1412, 1348, 1294, 1267, 1200, 1140, 1018, 980, 943, 903, 822, 735, 679 cm^{-1}; UV–vis (MeCN) λ/nm (log ε) 416 (sh, 3.91), 386 (4.29), 360 (sh, 4.11), 278 (sh, 3.90), 260 (4.21), 252 (4.23), 243 (sh, 4.13); MS (DEI, 70 eV) m/z (rel intensity) 586 ($M^+ + 2$, 32.99), 585 ($M^+ + 1$, 12.66), 584 (M^+, 100), 583 ($M^+ - 1$, 15.98), 582 ($M^+ - 2$, 86.30), 581 ($M^+ - 3$, 31.10), 580 ($M^+ - 4$, 51.93), 579 ($M^+ - 5$, 14.54), 578 ($M^+ - 6$, 21.40), 457 ($M^+ - I$, 89.66), 413 ($M^+ - C_2H_4O$, 13.20), 397 ($M^+ - C_2H_4O_2$, 5.58), 377 (25.03), 333 (18.94); Found: C, 22.80; H, 1.19%. Calcd for $C_{11}H_6O_2Se_2I_2$: C, 22.71; H, 1.04%.

2,6-Dicyanomethylene-4-ethylenedioxy-2,6-dihydrocyclopenta[2,1-*b*;3,4-*b*′]diselenophene (12). To a suspension of sodium hydride (55–65 wt %, 275 mg, about 6.9 mmol) in anhydrous THF (5 mL) was added dropwise a solution of malononitrile (45 mg, 0.687 mmol) in anhydrous THF at room temperature under argon atmosphere; then the reaction mixture was stirred for 10 min at room temperature. To this were added successively a solution of **11** (200 mg, 0.344 mmol) in anhydrous THF (10 mL) and [$Pd(PPh_3)_4$] (79 mg, 0.069 mmol). The reaction mixture was stirred for 2 h at 50 °C, and then stirred for 2 h at 60 °C. After cooling to room temperature, to this reaction mixture was added dropwise bromine (1 mL). Then the reaction mixture was poured into water, and the precipitate that separated out was collected by filtration and washed with water and then with acetone to give 2,6-dicyanomethylene-4-ethylenedioxy-2,6-dihydrocyclopenta[2,1-*b*;3,4-*b*′]diselenophene (**12**) (99 mg, 0.217 mmol, 67%). Further sublimation in vacuo (10^{-3} mmHg) at 300 °C gave pure **12** as a violet powder: mp > 300 °C; IR (KBr) 3053, 2216, 1728, 1576, 1506, 1350, 1321, 1242, 1213, 1115, 1028, 1003, 947, 879, 849, 746 cm^{-1}; UV–vis (CH_2Cl_2) λ/nm (log ε) 527 (4.94), 496 (4.83), 462 (sh, 4.45), 361 (sh, 3.61), 344 (3.70), 324 (3.74), 304 (sh, 3.61), 281 (4.01), 270 (4.05); MS (DEI, 70 eV) m/z (rel intensity) 458 (M^+, 1.71), 456 ($M^+ - 2$, 0.46), 414 ($M^+ - C_2H_4O$, 100), 412 ($M^+ - C_2H_4O - 2$, 83.99). Found: C, 44.70; H, 1.46; N, 12.23%. Calcd for $C_{17}H_6N_4O_2Se_2$: C, 44.76; H, 1.33; N, 12.23%.

2,6-Dicyanomethylene-4-oxo-2,6-dihydrocyclopenta[2,1-*b*;3,4-*b*′]diselenophene (CPDS-TCNQ). To a suspension of finely powdered **12** (100 mg, 0.276 mmol) in dichloromethane (100 mL) was added 70% perchloric acid (20 mL) at 0 °C. After vigorous stirring at the same temperature for 3 h, the reaction mixture was poured into ice-water. The precipitate that separated out was collected by filtration and washed successively with water and then with ethanol to give a crude product (72.6 mg). On the other hand, the filtrate was extracted with dichloromethane, and the dichloromethane extract was washed with aqueous $NaHCO_3$, water, and then brine, and dried over Na_2SO_4. Solvent evaporation from the extract gave another crude product (20.7 mg). The combined crude product was extracted using a Soxhlet apparatus with dichloromethane. Solvent evaporation from the extract gave 2,6-dicyanomethylene-4-oxo-2,6-dihydrocyclopenta[2,1-*b*;3,4-*b*′]diselenophene (CPDS-TCNQ) (89.5 mg, 0.218 mmol, 99%). Further sublimation in vacuo (10^{-3} mmHg) at 300 °C gave pure CPDS-TCNQ as a violet powder: mp > 300 °C; IR (KBr) 3037, 2212, 1724, 1496, 1448, 1319, 1238, 1211, 895, 758, 735 cm^{-1}; UV–vis (CH_2Cl_2) λ/nm (log ε) 554 (sh, 4.42), 524 (4.86), 493 (4.66), 460 (sh, 4.26), 356 (sh, 3.73), 318 (4.32), 304 (4.29), 283 (sh, 3.99); MS (DEI, 70 eV) m/z (rel intensity) 417 ($M^+ + 3$, 8.46), 416 ($M^+ + 2$, 28.80), 415 ($M^+ + 1$, 24.06), 414 (M^+, 100), 413 ($M^+ - 1$, 20.71), 412 ($M^+ - 2$, 87.65), 411 ($M^+ - 3$, 38.15), 410 ($M^+ - 4$, 59.04), 409 ($M^+ - 5$, 13.19), 408 ($M^+ - 6$, 15.91), 407 ($M^+ - 7$, 4.68), 406 ($M^+ - 8$, 6.03); HRMS m/z 413.8562 (M^+) (Calcd for $C_{15}H_2N_4OSe_2$: 413.8558).

Me_4N(CPDT-TCNQ)$_2$. Black needles, mp > 300 °C; IR (KBr) 2197, 1714, 1539, 1475, 1375, 1338, 1298, 1225, 1146, 1082, 1034, 949, 756 cm^{-1}. Found: C, 57.58; H, 2.32; N, 17.58%. Calcd for $C_{34}H_{16}N_9O_2S_4$: C, 57.45; H, 2.27; N, 17.73%.

Me_4P(CPDT-TCNQ)$_2$. Black needles, mp > 300 °C; IR (KBr) 2198, 1716, 1500, 1477, 1419, 1380, 1321, 1300, 1250, 1219, 1147, 1068, 980, 899, 756 cm^{-1}. Found: C, 56.17; H,

2.36; N, 15.10%. Calcd for $C_{34}H_{16}N_8O_2S_4P$: C, 56.11; H, 2.22; N, 15.40%.

$Me_4As(CPDT\text{-}TCNQ)_2$. Black needles: mp > 300 °C; IR (KBr) 2198, 1714, 1475, 1417, 1375, 1321, 1294, 1219, 1146, 1068, 1045, 1034, 926, 756 cm^{-1}. Found: C, 53.01; H, 2.18; N, 14.41%. Calcd for $C_{34}H_{16}N_8O_2S_4As$: C, 52.92; H, 2.09; N, 14.52%.

$Me_4Sb(CPDT\text{-}TCNQ)_2$(Acetone). Black needles, mp > 300 °C; Found: C, 49.97; H, 2.45; N, 12.67%. Calcd for $C_{37}H_{22}N_8O_3S_4$: C, 50.70; H, 2.53; N, 12.78%.

$Et_4N(CPDT\text{-}TCNQ)_2$. Black needles, mp > 300 °C; IR (KBr) 2200, 1716, 1477, 1439, 1392, 1340, 1301, 1248, 1227, 1173, 1147, 1070, 997, 953, 783 cm^{-1}. Found: C, 59.61; H, 3.14; N, 16.16%. Calcd for $C_{38}H_{24}N_9O_2S_4$: C, 59.51; H, 3.15; N, 16.44%.

$Me_4N(CPDS\text{-}TCNQ)_2$. Black needles, mp > 300 °C; IR (KBr) 2198, 1703, 1471, 1376, 1333, 1296, 1221, 1136, 1080, 949 cm^{-1}. Found: C, 45.24; H, 2.07; N, 13.76%. Calcd for $C_{34}H_{16}N_9O_2Se_4$: C, 44.85; H, 1.77; N, 13.85%.

$Me_4P(CPDS\text{-}TCNQ)_2$. Black needles, mp > 300 °C; IR (KBr) 2195, 1705, 1471, 1421, 1373, 1321, 1296, 1219, 1136, 1066, 980, 928 cm^{-1}. Found: C, 44.18; H, 1.98; N, 11.98%. Calcd for $C_{34}H_{16}N_8O_2Se_4P$: C, 44.61; H, 1.76; N, 12.24%.

$Me_4As(CPDS\text{-}TCNQ)_2$. Black needles, mp > 300 °C; IR (KBr) 2185, 1705, 1473, 1417, 1373, 1315, 1288, 1219, 1136, 1049, 926 cm^{-1}. Found: C, 42.66; H, 1.72; N, 11.55%. Calcd for $C_{34}H_{16}N_8O_2Se_4As$: C, 42.57; H, 1.68; N, 11.68%.

$Et_4N(CPDS\text{-}TCNQ)_2$. Black needles, mp > 300 °C; IR (KBr) 2197, 1705, 1471, 1389, 1371, 1335, 1292, 1219, 1171, 1136, 1070, 997, 927, 781 cm^{-1}. Found: C, 47.82; H, 2.63; N, 13.00%. Calcd for $C_{38}H_{24}N_9O_2Se_4$: C, 47.82; H, 2.53; N, 13.21%.

References

1 J. Ferraris, D. O. Cowan, V. V. Walatka, and J. H. Perstein, *J. Am. Chem. Soc.*, **94**, 948 (1973).

2 a) J. M. Williams, J. R. Ferraro, R. J. Thorn, K. D. Carlson, U. Geiser, H. H. Wang, A. M. Kini, and M.-H. Whangbo, "Organic Superconductors," Prentice Hall, New Jersey (1992). b) T. Ishiguro and K. Yamaji, "Organic Superconductors" Springer-Verlag Berlin, Heidelberg (1990). c) G. Saito, *Phosphorus, Sulfur Silicon Relat. Elem.*, **67**, 345 (1992).

3 A. Kobayashi, H. Kim, Y. Sasaki, S. Moriyama, Y. Nishino, K. Kajita, W. Sasaki, R. Kato, and H. Kobayashi, *Synth. Met.*, **B339**, 27 (1988); A. Kobayashi, A. Miyamoto, R. Kato, A. Sato, and H. Kobayashi, *Bull. Chem. Soc. Jpn.*, **71**, 997 (1998); R. Kato, Y. Kashimura, S. Aonuma, N. Hanasaki, and H. Tajima, *Solid State Commun.*, **105**, 561 (1998).

4 Y. Yamashita, T. Suzuki, T. Mukai, and G. Saito, *J. Chem. Soc., Chem. Commun.*, **1985**, 1044; T. Suzuki, C. Kabuto, Y. Yamashita, and T. Mukai, *Chem. Lett.*, **1987**, 1129; T. Suzuki, C. Kabuto, Y. Yamashita, G. Saito, T. Mukai, and T. Miyashi, *Chem. Lett.*, **1987**, 2285.

5 K. Yui, Y. Aso, T. Otsubo, and F. Ogura, *Bull. Chem. Soc. Jpn.*, **62**, 1539 (1989); K. Yui, H. Ishida, Y. Aso, T. Otsubo, F. Ogura, A. Kawamoto, and J. Tanaka, *Bull. Chem. Soc. Jpn.*, **62**, 1547 (1989).

6 K. Takahashi and S. Tarutani, *J. Chem. Soc., Chem. Commun.*, **1994**, 519; K. Takahashi and S. Tarutani, *Adv. Mater.*, **1995**, 639; K. Takahashi and S. Tarutani, *Synth. Met.*, **70**, 1165 (1995).

7 S. Tarutani, T. Mori, H. Mori, S. Tanaka, and K. Takahashi, *Chem. Lett.*, **1997**, 627.

8 E. Günther, S. Hünig, K. Peters, H. Rieder, H. G. von Schnering, J.-U. von Schütz, S. Söderholm, H.-P. Werner, and H. C. Wolf, *Angew. Chem., Int. Ed. Engl.*, **29**, 204 (1990).

9 For the preliminary report on CPDT-TCNQ, see: K. Takahashi and S. Tarutani, *Chem. Commun.*, **1998**, 1233, where CPDT-TCNQ was designated CPDT.

10 P. Jordens, G. Rawson, and H. Wynberg, *J. Chem. Soc. C*, **1970**, 273.

11 A. Hallberg, S. Liljefors, and P. Pedaja, *Synth. Commun.*, **11**, 25 (1981).

12 K. Deuchert and S. Hünig, *Angew. Chem., Int. Ed. Engl.*, **17**, 875 (1978); S. Hünig, *Pure Appl. Chem.*, **62**, 395 (1990); M. Horner and S. Hünig, *Angew. Chem., Int. Ed. Engl.*, **16**, 410 (1977).

13 The profile of the temperature dependence of the resistivity of the Me_4N salt at the temperature region from room temperature down to 130 K altered even slightly depend on the sample of the single crystal. However, all of the single crystals transferred to semiconductors below 130 K.

14 J. Yamaura, R. Kato, H. Tajima, S. Tarutani, and K. Takahashi, *Synth. Met.*, **103**, 2212 (1999).

15 T. Mori, A. Kobayashi, Y. Sasaki, H. Kobayashi, G. Saito, and H. Inokuchi, *Bull. Chem. Soc., Jpn.*, **57**, 627 (1984).

16 G. Gronowitz, I. Johnson, and A.-B. Hörnfeldt, *Chem. Scr.*, **7**, 111 (1975).